

Directionality is an inherent property of biochemical networks

Feng Yang, Feng Qi, and Daniel A. Beard

Biotechnology and Bioengineering Center, Department of Physiology,
Medical College of Wisconsin, Milwaukee, Wisconsin 53226, USA

(Dated: October 20, 2019)

Abstract

The current procedure for determining feasible reaction directions for large-scale metabolic network is less concrete and arbitrary to some degree. This work demonstrates that the reaction directionality, which is constrained by mass balance and thermodynamic constraints, is an inherent property of a given network. It shows that the solution space constrained by physiochemical constraints can be approximated by a set of linearized subspaces in which mass- and thermodynamic balance are guaranteed. The presented method potentially can be used to *ab initio* predict reaction directions of genome-scale networks based solely on the network stoichiometric matrix.

PACS numbers: 89.65.-s, 89.75.Hc, 87.23.Ge, 87.23.Kg

arXiv:q-bio/0701004v1 [q-bio.MN] 2 Jan 2007

Electronic address: dbeard@mcw.edu

Constraint-based approaches to analyze biochemical networks, such as Flux Balance Analysis (FBA) and Energy Balance Analysis (EBA), are widely applied to study genome-scale metabolic networks [1]. A successful set of procedures has been established for determining the metabolic reactions in a genome-scale model [2, 3]. However, the procedure for determining feasible reaction directions is less concrete and arbitrary to some degree [4, 5]. Yet the information on reaction directions is crucial to ensure that predicted reaction fluxes are physically feasible and obtained results are reasonable [6, 7].

The allowable reaction directions of a biochemical network are constrained by mass-conservation constraints and thermodynamic constraints, both arise from the stoichiometry of a given network [5, 6, 8, 9]. While the linear mass-conservation constraint is rigorously applied in many applications, the nonlinear thermodynamic constraint is not typically considered due to its implicit nonlinearity and NP-complete problem. Consequently, the flux distribution solely determined by the principle of mass-conservation may not be physically feasible in reality.

The thermodynamic constraint on biochemical networks is based on the second law of thermodynamics, for which physicist Lord Kelvin stated it as follows: "There is no natural process the only result of which is to cool a heat reservoir and do external work." In terms of biochemical reaction network, it can be interpreted as: "Each internal reaction with non-zero flux must dissipate energy." [7] In other words, there should be no flux in any reaction loops since no energy is consumed. To rigorously implement this constraint, a robust algorithm, which is based on a NP-complete computation of the elementary modes for a network, has been previously developed [10]. However, an appropriate algorithm for genome-scale networks has not been developed until now. Here, an algorithm for determining feasible reaction directions in large-scale networks is introduced and applied to biochemical network models of mammalian cardiomyocyte [11].

To illustrate the ab initio prediction of reaction directions, we first consider a toy reaction network (Fig. 1). In this network, external fluxes J_1 , J_{12} , and J_{13} are assumed to have sign pattern of [+ ; + ; +], with the arrows in the figure indicating the direction defined as positive. This set of predefined transport flux directions is specified as \mathcal{J} . For a given network (shown as Fig. 1) and known boundary conditions (\mathcal{J}) , the procedures to ab initio predict the reversibility of each flux are described as follows.

Mass-irreversible (MI) reactions For a flux vector \mathcal{J} to be feasible, mass balance

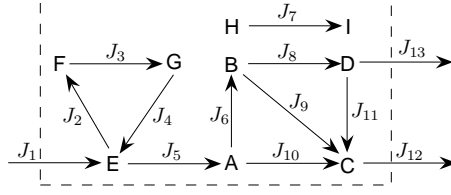


FIG .1: A toy network composed of 13 reactions (J_{1-13}) and 9 species (A through I). J_1, J_{12} and J_{13} are boundary fluxes that transport mass into and out of the system; J_2 through J_{11} are internal fluxes, as shown in the dashed box.

requires

$$d[A_i]/dt = \sum_j S_{ij} J_j = 0; \text{ and } \mathcal{J} \text{ obeys} \quad (1)$$

where S_{ij} is the stoichiometric coefficient of i th metabolite (A_i) in j th reactions, and J_j is the flux of reaction j . The reversibility of a flux (\mathcal{J}) that satisfies Eq. (1) can be found by computing the maximum and minimum allowable values given that the flux vector obeys the mass-balance. The feasible signs of mass-irreversible fluxes follow directly from the computed range ($J_j^{m_{ax}}, J_j^{m_{in}}$). The calculated results show $J_{2,4,6,8,11}$ are mass-reversible, J_5 is mass-irreversible and J_7 is mass-infeasible. Notably, we observe that J_5 is a strictly mass-irreversible (SM I) flux since exchange fluxes would be terminated if \mathcal{J} is close to zero. Such fluxes represent the backbone of the network; without them, the network would not function correctly.

Thermodynamic-irreversible (TI) reactions The constraints from the second laws of thermodynamics can be represented by the orthogonality of a flux vector \mathcal{J} against the sign patterns of the internal cycle space [7]. The reversibility of each flux that satisfies both mass-balance and thermodynamic constraints can be calculated with additional thermo-constraints

$$\begin{aligned} [J_j^{m_{ax}}; J_j^{m_{in}}] &= \text{optimum } (J_j); \text{ such that i) } S \mathcal{J} = 0; \\ \text{ii) } \mathcal{J} &\text{ obeys } \quad \text{iii) sign } (\mathcal{P})^? ; \text{ for each } 2 \leq C^?; \end{aligned} \quad (2)$$

where \mathcal{P} represents a flux vector that only includes the internal reactions; $C^?$ is a set of internal cycles of the oriented matroid associated with the null space of the stoichiometric matrix of the network; and \mathcal{P} are sign vectors with entries chosen from the set $\{0; +; -\}$. The reversibility satisfying thermo-constraints can also be obtained by scanning the complete set

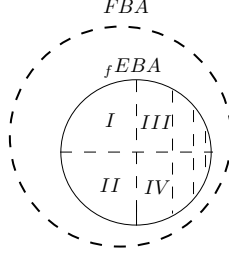


FIG. 2: Illustration of the solution space constrained by mass-balance only (FBA), the solution space constrained by nonlinear energy balance analysis (fEBA), and the linearized thermodynamic-feasible spaces (lEBA), i.e. solution space of I, II, III, IV, etc.

of external cycles (elementary modes) if it is calculable [10]. The results show that J_2, J_3 and J_4 are thermodynamically infeasible, J_6, J_8 and J_{10} are constrained to proceed in the positive direction only, and J_9 and J_{11} can achieve both maximum positive and minimum negative flux values and thus remain undetermined (i.e. reversible). Therefore, the necessary condition for thermodynamic feasibility of this network is M I [T I].

Sufficient condition (U I) for thermodynamic feasibility Although the irreversibility constraints identified so far (M I [T I) is sufficient to guarantee thermodynamic feasibility in certain cases [10], in general they are merely necessary and not sufficient to ensure a given network to be thermodynamically feasible. For example in the toy network, to be thermodynamically feasible one of the following additional linear constraints has to be included, I) If $J_9 > 0$, then J_{11} can be in any direction; II) If $J_{11} < 0$, then J_9 can be in any direction; III) If $J_9 < 0$, $J_{11} < 0$; IV) If $J_9 > 0$, $J_{11} > 0$, etc. The solution spaces constrained by these linear constraints, together with the constraints identified in Eq. (1,2), can be illustrated in Fig. 2.

Since the space defined by traditional FBA may not be physically feasible, the space of fEBA, in which both mass-balance and energy-balance are guaranteed, represents a better approximation of real network behaviors than using FBA only. Furthermore, while the inherent nonlinear thermodynamic constraint can be translated into to a set of linearized subspaces (lEBA), it is not practicable to enumerate a complete set of these subspaces (maximally $2^{n_{rev}}$ for n_{rev} reversible fluxes), especially for large-scale networks. To approximate the nonlinear fEBA space, however, it is possible to enumerate a limited set of subspaces (lEBA) in which the reversibility of the network is maximized. Thus, they represent the largest

sub-solution spaces of f_{EBA} , for example, the subspaces of I and II in Fig. 2. Therefore, the real network behavior could be maximally captured by studying these linearized subspaces. For those subspaces that are heavily constrained (such as the subspaces of III, IV and others), it is assumed that they represent non-typical network behaviors, or the time staying in these states is highly limited. Some related theorems have been observed in the above analysis.

Theorem 1 Mass-irreversible reactions are not reducible by thermodynamic constraints. Suppose a MI reaction that connects species A to B, $A \rightarrow B$, is reduced as thermodynamically infeasible by a directed loop of L. As a result, there must be a pathway that connects A to B along a reversed loop of L by the definition of the mass balance. The existence of such a reversed loop thus disables the reducibility of the directed loop L, and no thermodynamically infeasible loop exists between the species A and B. This theorem implies $MI \setminus TI = \emptyset$, and also indicates that if a reaction is suspected to be TI (due to incomplete cycle calculation or non-guaranteed global optimization), one of optimum values (J^{max} or J^{min}) of this reaction must be zero. Otherwise, it is a strictly mass-irreversible (sMI) reaction which is guaranteed to be detected by mass-balance analysis.

Theorem 2 Mass-reversible reactions can be reduced as thermodynamically infeasible and thermodynamically irreversible. Supposing a reversible flux $J_i, A \rightleftharpoons B$, involved in a loop L, then all reactions in this loop L must be reversible because of the connectivity between A and B along L. To block this infeasible reaction loop, any reversible reactions can be chosen and reduced as irreversible. Therefore, the loop constraints are active with respect to the reversible flux J_i , which can be reduced as thermodynamically infeasible (such as $J_{2,4}$), or reduced as thermodynamically irreversible (such as $J_{6,8,10}$) in the toy network model.

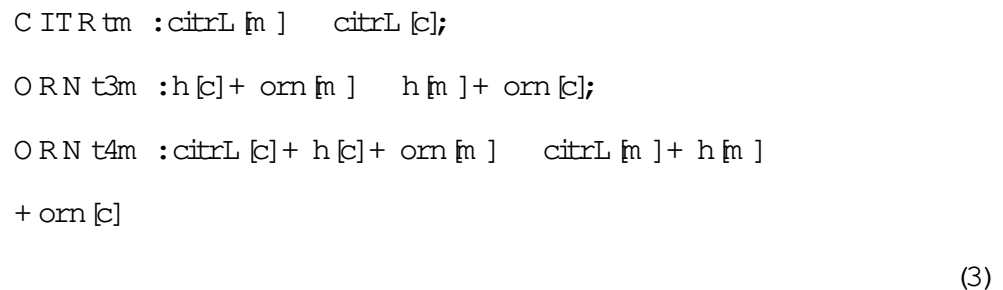
Theorem 3 A directed cycle in which all reactions are irreversible is impossible. Suppose there is a directed cycle which contains an irreversible flux, $A \rightarrow B$ and a set of irreversible reactions along loop L, then the reactions along loop L must be reversible by mass-balance. Therefore, a full directed cycle is impossible and any cycle can always be eliminated by assigning directions to some reversible reactions in the network. Furthermore, it also indicated the number of reversible reactions in any cycle must be in the range of $[1, n]$, where n indicates the total number of fluxes in the network. While an individual cycle requires at least one direction assignment to block, for a network with n_{cyc} cycles, maximally it could require n_{cyc} assignments. The more complex of a network, the

larger number of cycles, and the larger number of assignments are needed. Consequently, thermodynamic impacting factor (TIF), which is the ratio of the number of TFI [UI and the total number of nonzero fluxes, could be possibly used to evaluate the complexity (robustness) of a given network and to quantitatively determine the thermodynamic impacts on the traditional FBA.

The developed methodology has been applied for the metabolic network of mammalian cardiomyocyte [11] which accounts for 240 metabolites and 257 reactions. While the stoichiometric structure of this model has been adopted, the flux direction previously assigned are typically ignored. Particularly, we define a network in which the directions of boundary fluxes are assigned based on the published model, but all internal reactions, except two fluxes of ATP hydrolysis and a transport flux of 12DGRt2, are assumed to be reversible. In this network model, three transport fluxes are constrained to operate in the direction of net uptake of substrate (glucose, oleate and oxygen uptake) and 28 transport fluxes (including CO₂, acetate and 26 additional output fluxes) are constrained to operate in the direction of net production of reactant. A total of 33 reaction directions are specified and 219 internal reaction directions are computed.

With these 33 irreversibility constraints, mass-balance analysis identifies 18 SMI internal fluxes (see red and blue fluxes in Fig. 3), which represent an essential reaction set for this network. It also shows that only 14 products (of 32 desired metabolites), could be possibly produced from the sources (i.e. glucose, oleate, and O₂), with the aids of three reversible transport fluxes of CO₂, H⁺, and H₂O. In addition, 70 mass-infeasible fluxes, 57 mass-irreversible fluxes, and 74 mass-reversible fluxes are identified.

The results from intensive samples (559,518,687 external cycles) further show that three mass-reversible fluxes (CITR_{tm}, ORN_{t3m}, ORN_{t4m}) are thermodynamically infeasible. In particular, we observed that these three reactions:



develop a reaction cycle as CITR_{tm} + ORN_{t4m} - RN_{t3m} = 0. It is also found that h[c] is

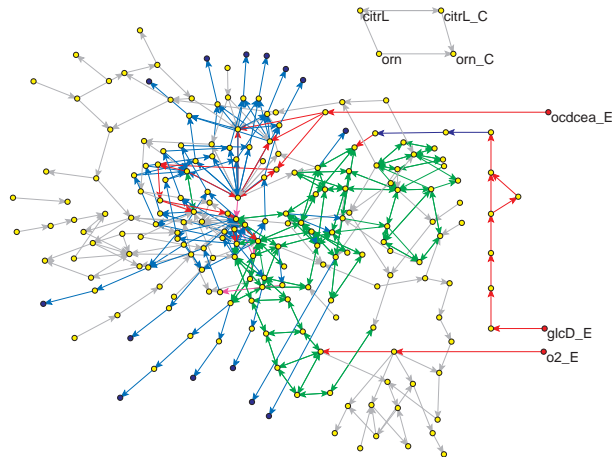


FIG. 3: Illustration of a thermodynamically feasible network of the cardiomyocyte network. The nodes and edges represent metabolites and reactions, respectively. In particular, the red, blue and yellow nodes represent the sources, the sinks and the intermediate metabolites of the network, respectively. Red edges and blue edges represent the strictly mass-irreversible reactions, and violet red edges and navy blue edges represent mass-reversible reactions. In particular, reactions in red or violet red proceed in the same direction as the definition of the network; reactions in blue and navy blue proceed in a reversed direction. An infeasible reaction cycle is shown at the right top corner of Fig. 3. For simplicity, the currency of the biochemical networks, such as ATP, ADP, P_i, NADH, NAD, H⁺, H₂O and CO₂, have not been shown.

the only metabolite that connects this reaction cycle to the remaining part of the network, which remind of the reaction cycle $J_2 \rightarrow J_3 \rightarrow J_4 \rightarrow J_2$ in the toy network. Thus neither direction is feasible for all these three reactions. In addition, 74 mass-reversible fluxes are found to be thermodynamically-reversible and no thermodynamically-irreversible flux is found.

The solution space constrained by M I [T I needs to be further refined since 1099 infeasible cycles are still embedded in this network. However, by specifying only 14 reversible fluxes (out of 74 reversible fluxes) be irreversible, it is possible to eliminate all those infeasible cycles. A final thermodynamically-feasible network for mammalian cardiomyocyte has been illustrated in Fig. 3, which consists of 91 infeasible reactions, 92 irreversible reactions and 74 reversible reactions. However, such a linearly constrained subspace is not unique, as indicated in the toy network. To further explore the nonlinear thermodynamically-feasible space, a large number of subspace (see Fig. 4) has been generated by assigning directions to those reversible fluxes. Notably, each irreversibility assignment is generated in such a way that

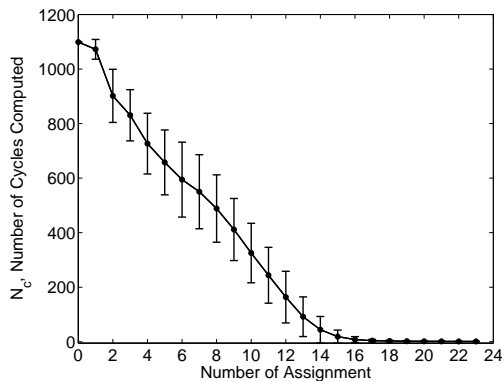


FIG. 4: Demonstration of reductions in the number of cycles with extra irreversibility constraints (UI). It represents the results of 10^5 independent simulations for generating T-feasible solution spaces. Bars represent the standard deviation of the number of cycles that are eliminated at each particular assignment.

the maximum number of infeasible cycles can be eliminated. Therefore, the generated set of linear constraints represents the minimal requirements for a given network being mass- and thermodynamically feasible, and thus represents the largest linear subspaces in Fig. 2.

Surprisingly, the computed thermodynamically feasible irreversibility constraints (see supplementary material) show significant difference when compared to the original assigned directions, by which the space defined is not thermodynamically feasible (7 thermodynamically infeasible cycles are still included). To make it physically feasible, three mass-reversible fluxes (CITR_{tm}, ORN_{t3m}, ORN_{t4m}) have to be eliminated, and at least one additional direction assignment, either specifying AKGMAL_{tm} (previously assigned as reversible) be positive or specifying ASPTA_m be negative, has to be added into the original definition of the network. Although these additional constraints did not invoke significant impact on the overall results from [1], it does change the flux distribution with the given boundary fluxes.

While the final network revised from the original definition represents a special case of mass- and thermodynamically balanced network, it is significantly different from the network which shows the maximum level of flexibility (i.e. containing the maximum number of reversible reactions). Table 1 shows the difference between a sampled network (Fig. 3), which represents one of the largest subspaces of mass- and thermodynamically balanced, and the original definition of the network, with flux balance analysis (FBA) and with revision from T-constraints. The significant difference between this ab initio prediction and the previously assigned directions,

TABLE I: Comparison of T-networks with high flexibility and the original network as well as mass-balanced network and thermodynamically balanced network.

| | P I ^a | P I+ FBA | P I+ FBA + EBA | EBA ^b |
|---------------------|------------------|----------|----------------|------------------|
| Infeasible fluxes | 0 | 149 | 149 | 91 |
| Positive [3] fluxes | 156 | 60 | 61 | 34 |
| Negative [3] fluxes | 3 | 21 | 21 | 58 |
| Reversible fluxes | 98 | 27 | 26 | 74 |

^aP I indicates the directions originally assigned by Vo and Palsson [11]; P I+ FBA and P I+ FBA + EBA indicate the original assignment is imposed on additional constraints from mass-conservation and thermodynamic feasibility.

^bA T-feasible network corresponds to the network shown in Fig. 3

^cThe positive reaction direction is defined based on the left-to-right reaction direction in the original model definitions [11]

may be explained by the fact that mass-conservation and thermodynamic constraints are not the only constraints that a network must satisfy. The non-identified limits may come from gene regulatory constraints, topological constraints, environmental constraints [12], and constraints that are accumulated from evolution and natural selection. By systematically studying the difference between the results from ab initio prediction and the experimental observation, we may find some interesting knowledge 'gap', and consequently improve the further predictions on the flux distributions.

In this presented work, a biophysical constraints is applied to the genome-scale biochemical network for computing flux directions and determining a linear constrained mass- and thermodynamically-balanced solution space. Given a reaction network and a set of prior constraints on certain flux directions (such as known transport flux directions) the algorithm determines a minimal set of irreversibility constraints (reactions directions) that is sufficient to guarantee thermodynamic feasibility. The developed methods could be used as a tool to systematically design a biochemical network, greatly facilitate the further Flux Balance Analysis and Energy Balance Analysis, improve their predictions of the flux distribution, and help capturing the real physically meaningful behavior of the network studied. Numerically,

a linear solution space will make flux optimization more reliable and efficient.

- [1] A. R. Joyce and B. O. Palsson. The model organism as a system : integrating 'omics' data sets. *Nat Rev Mol Cell Biol*, 7:198{210, 2006.
- [2] J. Forster, I. Famili, P. Fu, B. O. Palsson, and J. Nielsen. Genome-scale reconstruction of the *saccharomyces cerevisiae* metabolic network. *Genome Res*, 13:244{53, 2003.
- [3] C. Franke, R. J. Siezen, and B. Teusink. Reconstructing the metabolic network of a bacterium from its genome. *Trends Microbiol*, 13:550{8, 2005.
- [4] Kummel A, Panke S, and Heinemann M. Systematic assignment of thermodynamic constraints in metabolic network models. *BM C Bioinformatics*, 7:512{, 2006.
- [5] N. D. Price, I. Thiele, and B. O. Palsson. Candidate states of *helicobacter pylori*'s genome-scale metabolic network upon application of. 2006.
- [6] D. A. Beard, S. D. Liang, and H. Qian. Energy balance for analysis of complex metabolic networks. *Biophys J*, 83:79{86, 2002.
- [7] D. A. Beard, E. Babson, E. Curtis, and H. Qian. Thermodynamic constraints for biochemical networks. *J Theor Biol*, 228:327{33, 2004.
- [8] J. M. Lee, E. P. Gianchandani, and J. A. Papin. Flux balance analysis in the era of metabolomics. *Brief Bioinform*, 7:140{50, 2006.
- [9] C. S. Henry, M. D. Jankowski, L. J. Broadbelt, and V. Hatzinikitis. Genome-scale thermodynamic analysis of *escherichia coli* metabolism. *Biophys J*, 90:1453{61, 2006.
- [10] F. Yang, H. Qian, and D. A. Beard. A *bio* prediction of thermodynamically feasible reaction directions from biochemical network stoichiometry. *Metab Eng*, 7:251{9, 2005.
- [11] T. D. Vo and B. O. Palsson. Isotopomer analysis of myocardial substrate metabolism : A systems biology approach. *Biotechnol Bioeng*, 2006.
- [12] B. O. Palsson. *System Biology*. Cambridge University Press, 2006.